Joint Int. Conf. on Math. Methods and Supercomp. in Nuc. Appl., April 19-23, 1993, Karlsruhe, Germany,
Proc. Ed. H. Küsters, E. Stein, W. Werner, Kernforschungszentrum Karlsruhe, 1993, Vol.1, pp. 236 - 247

# ANALYSIS OF FLOW MECHANISMS IN RAYLEIGH-BÉNARD CONVECTION AT SMALL PRANDTL NUMBERS

G. Grötzbach, M. Wörner
Kernforschungszentrum Karlsruhe
Institut für Reaktorsicherheit
Postfach 3640, D-7500 Karlsruhe
Germany
Tel. 07247/824477

## ABSTRACT

The results of direct numerical simulations of Rayleigh-Bénard convection in sodium and air are investigated regarding the dominant flow mechanisms. The dynamics of these mechanisms in both fluids are analysed by means of computer generated movies. All simulations for sodium are beyond the transition range from laminar to turbulent convection as denoted by stability diagrams. Nevertheless, regular roll like structures are found which are more and more distorted threedimensionally with increasing Rayleigh number. All sodium flows considered show indications for a fly-wheel type of vortex rotation. At small scales the velocity fields show structures comparable to those found in air at the same Grashof number. In the simulation for air large spoke pattern systems with only a few plume centres are found which are similar to those observed in earlier simulations for smaller Rayleigh numbers. This simulation still belongs to the regime of soft turbulence. The results for both fluids are used to conclude on the relevance of the mechanisms found for the development of turbulence models.

## INTRODUCTION

In new fast breeder designs the after heat removal in accident situations shall be achieved by pure natural convection. To analyse the corresponding flow phenomena and temperature transients, experiments are performed in scaled reactor models with water[1,2]. The interpretation of the experiments and the transfer of the results is mainly done by computer codes[3,4]. The turbulence models needed and used in such codes have to be improved to be applicable to purely buoyant flows. One effort in this context is to determine turbulence data to calibrate existing models, e.g. from experiments[5,6] or from direct numerical simulations[7,8]. A complementing effort is to gain a better understanding of the physical mechanisms in this type of flow to allow for the development of improved turbulence models.

The mechanisms in natural convection of liquid metals are mainly investigated in simple geometries, like the Rayleigh-Bénard convection, which is the convective upwards directed heat transfer through a large horizontal fluid layer enclosed between two plane walls. An influence of the type of fluid on the heat transfer through such fluid layers has to be expected because of counteracting physical phe-

nomena. In liquid metals ($Pr = \nu/\kappa << 1$, Pr = Prandtl number, $\nu$ = viscous diffusivity, $\kappa$ = thermal diffusivity) the heat transfer by molecular conduction will be dominant to much larger heating rates than in fluids with small thermal diffusivity like water etc. ($Pr > 1$). On the other hand liquid metals have small viscosities and would therefore allow for stronger convective contributions to heat transfer than highly viscous fluids ($Pr >> 1$). Accordingly one finds in experiments at large Prandtl numbers that the flow development extends over more than three orders of magnitudes in Rayleigh number ($Ra = g\,\beta\,\Delta T_w\,d^3/(\nu\kappa)$, g = gravity, $\beta$ = volume expansion coefficient, $\Delta T_w$ = temperature difference between both walls, d = distance between walls). The flow develops from no motion at small heating rates ($Ra < Ra_{cr} = 1708$) over steady two-dimensional and three-dimensional flows, over time-dependent three-dimensional flows, to fully turbulent flows at large heating rates. At Prandtl numbers around one, the fully turbulent regime itself is subdivided in a regime with soft and hard turbulence, each one showing its own statistical features[9]. With liquid metals the transition from no motion to irregular flow extends only over a range of Rayleigh numbers being apart less than a factor of two[10]. This very different behaviour was also predicted theoretically[11]. Thus one finds in liquid metals at small Ra very irregular or turbulent convection, but the heat transfer rate does only show considerable convective contributions at much larger heating rates ($Ra > 10^4$)[12,13]. In this range a flywheel-type of convection is predicted by two-dimensional methods to occur[14] but experimentally it is found even at smaller Rayleigh numbers[15]. Currently there are no extensive field data available from experiments which could help to reproduce the detailed characteristics of the flow field at any Rayleigh number in liquid metals which is necessary to gain a better understanding of the flow mechanisms.

In this paper we will analyse a database of about 10 Gigabytes created by the method of direct numerical simulation of the fully 3d and time-dependent convection in sodium for Rayleigh numbers from 3,000 to 24,000[7,8] and in air for Ra = 630,000. The simulations were performed mainly to study statistical results of turbulence, to deduce assumptions for improved turbulence models, and to determine values for model coefficients suited to natural convection in liquid metals. Detailed statistical results for some turbulence assumptions are given in[8] at this conference. Here we use filtering and graphical tools on a main frame computer and current tools on a graphic workstation to deduce details for the structures in these flows, show their dynamics by means of computer generated movies, and show the very different length scales occurring. The results allow for conclusions on the future strategy to improve existing turbulence models for this type of flow.

## SIMULATION METHOD AND ANALYSING PROCEDURE

The simulation model used is the TURBIT-code[16]. It is based on the complete three-dimensional time-dependent conservation equations for mass, momentum, and thermal energy for a Newtonian fluid. The validity of the Boussinesq approximation is assumed. The code uses a finite difference scheme on a staggered grid in space. Recently the code was extended by a semi-implicit time-integration scheme[17]. Using modified direct Poisson solvers to solve the resulting sets of linear equations, for details see[17], improves considerably the efficiency of these simulations. Here we use sufficiently fine grids and large aspect ratios so that all scales of turbulence are resolved and no turbulence assumptions are required. Thus, no subgrid scale models and no wall laws are necessary. This means, there are no empirical parameters in the numerical model except for the dimensionless numbers Ra and Pr characterising the flow and the grid data.

Essential parameters are the data specifying the grid. The number of equidistantly spaced mesh cells in each horizontal direction is up to $N_1 = N_2 = 250$, and in the non-equidistantly spaced vertical direction up to $N_3 = 39$, Tab. 1. Periodic boundary conditions are used in the horizontal directions to simulate an infinite channel. The horizontal extension has to be chosen to record all large scale phenomena. Unfortunately there is no information available form experiments or theory to choose aspect ratios for Rayleigh numbers above the critical one for liquid metals. From simulations on a coarse grid for Ra = 6,000 using horizontal extensions $X_i/d$ (i = 1,2) from 4 to 16 we found, that the large scale features of the flow simulated for aspect ratios of 8 and greater are independent on the aspect ratio. Therefore we used 8 for sodium and, because of the initial data available, 7.92 for air. For verification of the code and of these grid specifications see[7,8,17].

Initial conditions are gained on three different ways. We either use zero velocities and random temperature fluctuations superimposed to a schematic piece wise linear vertical profile of the mean temperature. This method avoids problems of transferring especially regular flow patterns from small Rayleigh numbers to larger ones where such patterns might remain but might physically not exist. Or we use simulation results on the same grid for a smaller Rayleigh number, or we start from simulation results for the same Rayleigh number gained on a coarse grid and interpolate quadratically to a finer grid. Both latter methods turned out to allow for reductions of CPU-times by one order of magnitude or more compared to runs starting from more or less random data on the required fine grid. The CPU-times given in Table 1 are those on the finest grids only.

The code was run on a VP400-EX for Rayleigh numbers from 3,000 to 24,000 in sodium using grids with up to 2.5 million mesh cells to create a data base for Rayleigh-Bénard convection mainly for statistical analysis of turbulence data, Tab. 1. In two cases all simulated 3d data were stored in short time intervals so that the dynamics of the flow and temperature field could be analysed by creating computer generated movies. The filtering out of data to be visualised was performed on an IBM 3090 VF by scanning up to 5 Gigabyte of data for each scene.

For the liquid metal flow the DISSPLA-software was used in batch-mode on the IBM to create coloured contourline figures of horizontal and vertical cuts through the temperature field e.g. The graphical information stored in CGM-files of about 45 Megabyte was interpreted on a central Stardent workstation GS 2000 and finally stored on a digital real-time disk. In using DISSPLA we were confronted by several serious DISSPLA-internal problems. Meanwhile some of these are solved by module updates.

For the air flow considered for comparison purposes the data for the temperature and the vertical velocity component in only one quarter of the channel were converted on the IBM to the format for the AVS software. The resulting data of 720 Megabyte were visualised in a semi-interactive mode by means of AVS on a local GS 2000 in form of three-dimensional isosurfaces of temperature and superimposed to it the colour coded values of the local vertical velocities. These figures were stored as pixmaps with about 1.1 Gigabyte. These finally were re-interpreted on a central GS 2000 and stored on a real-time disk. The CPU-times needed in this latter case for simulation, for filtering out data, for visualisation on the workstation, and for transfer of data by FTP on ETHERNET are each in the order of some 10 hours. This way of movie production needs much more effort for file handling, but this is mainly because of the three-dimensional presentation chosen instead of the two-dimensional one chosen with DISSPLA. This procedure is highly flexible

as regards to the kind of presentation, because the same input files for AVS can be used for any 3d or 2d visualisations.

## FLOW STRUCTURES IN LIQUID SODIUM

The isosurface for a temperature of 1/2 ($T_{w1} + T_{w2}$) at the smallest Rayleigh number Ra = 3,000, shows only very small distortions by convection having large length scales, Fig. 1. The small upwards and downwards directed distortions in the isosurface are caused by the upward (red) and downward (blue) movement of the fluid which shows somewhat smaller scales than the temperature field. The flow obeys systematic roll-like structures which have only slight three-dimensional distortions. Considering isosurfaces of small positive vertical velocities (with colour coded temperatures, red = hot, blue = cold) clearly visualises these rolls, Fig. 2. A phenomenon which was not observed up to now at other Prandtl numbers is the existence of small areas of upward flow near the upper wall in the area in which the downward flow is dominant and vice versa. This is due to the existence of small secondary roll like structures near both walls, Fig. 3. This can be interpreted as an indicator for the existence of a kind of fly-wheel or solid body rotation of the vortex rolls. Thus, in the fully three-dimensional simulation we find the fly-wheel convection for the roughly two-dimensional flow as it was proposed theoretically for larger Rayleigh numbers ($Ra > 5 \cdot Ra_{cr}$, where $Ra_{cr} = 1{,}708$)[14], but it occurs at much smaller Rayleigh numbers. This result of the simulation is in accordance with experimental results showing inertial convection at $Ra > 1.08 \cdot Ra_{cr}$)[15].

Comparable presentations of the numerical results for Ra = 12,000 and similarly for Ra = 6,000 still show large roll like structures, mainly indicated by the vertical deformation of the isosurface for the temperature, Fig. 4. Here we find much stronger three-dimensional distortions. The colour code for the velocity demonstrates that the velocity field is much more irregular than the temperature field and obeys much finer scales. A new phenomenon is the existence of spoke pattern like connections across rolls, best to be recognised in the isosurface for a small positive value for the vertical velocity, Fig. 5. These spoke patterns do not only exist near the lower wall, but also at the upper wall because here we find a very rugged isosurface. On the other hand the small secondary currents indicating fly-wheel rotation of the large vortices still exist. In a pure fly-wheel type of convection there is no convective heat transfer within the vortices. Here the three-dimensional distortions of the vortices enforce a thin outer layer in each vortex in which the heat penetrates by convection. By this mechanism the heat transfer rate will be increased with increasing three-dimensionality. In general the velocity field at this Rayleigh number obeys much smaller scales as the temperature field.

From a similar presentation for Ra = 24,000 one would conclude that there are no more roll-like structures existent, Fig. 6. The pillow-like structures are due to the upwelling plumes, hitting the upper wall and expanding horizontally. The spatial arrangement indicates an irregular distribution of local plume centres. Nevertheless a statistical analysis at midplane shows that the flatness of the temperature field in all cases is nearer to 1.5, which is the value for a sinusoidal distribution, than to 3, which holds for Gaussian distributions, Tab. 2. This means, the roll-like structures are still dominant. The macroscopic wavelengths given in Tab. 2 for the rolls are rough estimates from contourline plots of velocities and temperatures and from analysing two-point correlations. As we found that for simulations with sodium an aspect ratio of $X_i/d = 8$ is required, this indicates that about $X_i \approx 3 \cdot \lambda$ is sufficient for adequate simulations in this range of Rayleigh numbers. This re-

quirement for the horizontal periodicity lengths is stronger than in air where in many simulations $X_i \approx 2\,\lambda$ was used in the turbulent regime. The reason might be that here still regular structures are dominant causing a horizontal coupling by convection over larger horizontal distances, and that the tremendous thermal conductivity causes also a strong horizontal coupling.

The dynamics of the fields for Ra = 12,000 are analysed and discussed on the basis of a movie. The vertical cuts through the temperature fields and the temperature fluctuation field at any position show only weak local distortions indicating areas with updrafts and downdrafts. Changes in this field are very slow. In contrast, the vertical cuts through the field of kinetic turbulence energy show very fast rotation of rolls. These differences in the time scales of the velocity and temperature fields are in accordance with the differences in their length scales, see spectra given for these simulations in[8]. The roughly linear energy distribution within the rolls is an additional indicator for the fly-wheel or solid body rotation.

## FLOW STRUCTURES IN AIR

The simulation for air was performed for verification purposes and to study the influence of the molecular Prandtl number on the statistics and on the mechanisms of turbulence. The isosurface for a temperature value of $T = 0.7$ ($T_{w1} = 1$, $T_{w2} = 0$) is given in Fig. 7. Here no roll-like structures exist, instead plumes with upward movement e.g. concentrate in knot-like structures. In some plumes the hot fluid rises from the lower wall to the cold upper wall. The plumes are horizontally connected by thin spoke patterns of slow upward movement existing only in a thin near-wall layer. The vertical velocities indicated by the colour code have the same spatial scales as the temperature field because the Prandtl number is near one.

The structures found in this simulation have earlier been found in different numerical simulations at this Prandtl number at a smaller Rayleigh number[18,19], but up to now they have not been shown in experiments at the same Prandtl number. At larger Prandtl numbers they have been shown to exist in the near wall range[20]. Statistical analysis of the features of these structures show, that the macroscopic wavelength $\lambda$ is somewhat greater than in the earlier simulation for a smaller Rayleigh number, Tab. 2. The value of $\lambda$ justifies the use of such large aspect ratios. Especially to achieve correct values for the Nusselt number turned out to require large aspect ratios at these Rayleigh numbers. The value for the flatness of the temperature fluctuations at midplane shows quantitatively that there are no roll-like structures existent or superimposed. The values are nearer to 3, this means Gaussian distribution, than to 6, which means exponential distribution. The latter one is expected for hard turbulence. This means our simulation belongs to the upper end of the soft turbulence regime, or because the flatness is greater than 3, to the transition range between both states defined by the Chicago group[9].

The dynamics of this flow is also analysed by means of a movie. Sections through the temperature field and three-dimensional presentations of isosurfaces for several temperature values are used for presentation in one quarter of the channel only. This reduction of data had to be chosen because of the poor resolution of the S-VHS video tape facilities. The spoke pattern like structures are attracted by the few dominant plume areas. By withdrawing spokes, larger cells are formed. Within these calm areas new spokes develop due to local Rayleigh-Taylor instabilities. Some of the spokes are pushed away by plumes arriving from the opposite wall, hitting the wall considered, and redistributing the fluid in the wall layer horizon-

tally. This feeds the few plume areas. The plumes don't appear regularly, but some plume areas move slowly in the horizontal direction. Some plumes merge and may form new knot-like plume centres. The time-scale of the movie is about that of real-time in Deardorff's experiment[21]. The dynamics of the flow found here is comparable to that found at a smaller Rayleigh number[19].

## CONCLUSIONS

To investigate the flow mechanisms in Rayleigh-Bénard convection of sodium and air an existing data base resulting from direct numerical simulations is analysed mainly by graphical tools. At small Rayleigh numbers the temperature field in sodium appears to be rather smooth or laminar. It is only slightly distorted by the velocity field at large wavelengths. Even in the turbulent regime it shows the existence of roll-like structures. Small secondary vortices may be a consequence of solid body rotation of the large vortex rolls. An other indicator for inertial convection might be found in the flatness values for the temperature fluctuations at midplane which indicate roughly sinusoidal distributions despite rather randomly appearing velocity fields. This numerical result is in contrast to theoretical predictions using 2d methods, but it agrees with the conclusion from experiments that inertial convection exists at these Rayleigh numbers.

The velocity field behaves completely different. It extends from large to very small scales. Spoke pattern like structures are found at larger Rayleigh numbers as they also exist in convection of fluids with Prandtl numbers near unity or greater. Thus the velocity field shows similarities at small scales for all Prandtl numbers. Indeed, the Grashof number $Gr = Ra/Pr$ which may be used for scaling the velocity field is about the same in all our simulations, Tab. 1. The macroscopic wavelengths found in sodium at these Rayleigh numbers are rather small so that a rough similarity at large scales can be expected with those in air at comparable Rayleigh numbers. Nevertheless, the macroscopic wavelength is no measure for estimating how far the flow is correlated in the horizontal directions, because such correlations are observed over larger distances.

The dynamics of the mechanisms in the simulation for air is qualitatively the same as in an earlier published simulation for a smaller Rayleigh number. Especially the flatness values indicate that both flows can be classified as soft turbulence. This is in accordance with the classification by the Chicago group. The large aspect ratio used here allows to conclude on the macroscopic wavelength of the velocity field. Obviously it still depends on the Rayleigh number even at these levels. It comes near to the value of the aspect ratio used often in simulations elsewhere. This may be one of the reasons why the calculated Nusselt number is too large in some of the published simulations.

Some of the features found in the convection layers with both fluids can be used to consider carefully terms in turbulence models using transport equations for turbulence quantities, like in the k-ε model and to select model assumptions for improved modelling of natural convection in liquid metals. As a consequence of the Grashof analogy of the velocity field at small scales we have to expect no problems with those terms in turbulence models describing small scale phenomena, like the dissipation, but due to the dominance of large scale ordered structures we may expect difficulties with terms describing large scale phenomena. A special problem of modelling these flows is the formulation of boundary conditions in all those calcu-

lations, in which the viscous and conductive wall layers can not be resolved. The problem with the not well known wall laws could partly be circumvented by using locally laws for turbulent shear flows. The reason is that the horizontal redistribution of the fluid along walls enforced by the plumes hitting the walls dominates the convective heat transfer from and to the walls.

In considering the computational effort to perform this study we are on the simulation side at the limits of our vector machine as regards to storage and tolerable CPU-times. Of course, faster and larger supercomputers will allow for simulations of higher turbulence levels which are more of technical relevance. The real bottle neck of this investigation was on the analysing side, especially as regards to the times needed for file transfer and visualisation in preparing the movies. DISSPLA turned out to be a somewhat problematic graphical tool, but when it is adequately implemented and it is operable, it is easy to handle. AVS is a highly flexible tool for interactive visualisation. It needs more effort for file handling when three-dimensional presentations shall be used in the movie. Two-dimensional presentations can be achieved very easily. The capability of presenting such a movie on the screen of a workstation is an additional advantage of this software. Therefore we meanwhile implemented in our code an interface to AVS for two-dimensional time-dependent presentations of any variable in a plane at any position in the channel. This turned out to be an attractive tool not only for presentation purposes, but also for daily analysis of simulation results.

## ACKNOWLEDGEMENTS

We gratefully acknowledge the work of F. Bösert and F. Leopold for implementing the DISSPLA software and of E. Hesselschwerdt for developing the interfaces to AVS and adapting AVS modules.

## REFERENCES

1 K. Satoh, H. Miyakoshi, "Study of decay heat removal by natural circulation," Proc. of the 4th International Topical Meeting on Nuclear Reactor Thermal Hydraulics (NURETH-4), Karlsruhe, Germany, (1989), pp. 378-383, Verlag G. Braun, Karlsruhe.

2 H. Hoffmann, H. Kamide, K. Marten, H. Ohshima, D. Weinberg, "Investigations on the transition from forced to natural convection for the pool type EFR in the 3d RAMONA model," Int. Conf. on Fast Reactors and Related Fuel Cycles, Oct. 28 - Nov. 1, 1991, Kyoto.

3 H. Ninokata, "Advances in computer simulation of fast breeder reactor thermalhydraulics," Proc. Conf. on Supercomputing in Nuclear Applications, Mito, Japan, (1990), pp.80-85.

4 H.A. Borgwaldt, "CRESOR, a robust vectorized Poisson solver implemented in the COMMIX-2(V) thermal-hydraulics code," Proc. Conf. on Supercomputing in Nuclear Applications, Mito, Japan, (1990), pp. 346-351.

5 J.H. Knebel, L. Krebs, U. Müller, "Experimental investigation of turbulent mixed convection in liquid sodium flow", NURETH-6, Grenoble, 1993.

6 D. Suckow, "Experimentelle Untersuchungen turbulenter Mischkonvektion im Nachlauf einer punktförmigen Wärmequelle", Dr. thesis, University Karlsruhe, 1993.

7 G. Grötzbach, M. Wörner, "Analysis of second order transport equations by numerical simulations of turbulent convection in liquid metals," Proc. of the 5th International Topical Meeting on Nuclear Reactor Thermal Hydraulics (NURETH-5), Salt Lake City, USA, Sept. 21-24, 1992, Vol. II. pp. 358-365, American Nuclear Society, LaGrange Park, Ill. 1992.

8 M. Wörner, G. Grötzbach, "Contributions to turbulence modelling of natural convection in liquid metals by direct numerical simulation," This conference.

9 F. Heslot, B. Castaing, A. Libchaber, "Transition to turbulence in helium gas," Phys. Rev. A36, 1987, pp. 5870-5873.

10 R. Krishnamurti, "Some further studies on the transition to turbulent convection," JFM 60, 1973, 99. 285-303.

11 R.M. Clever, F.H. Busse, "Convection at very low Prandtl numbers," Physics of Fluids, A2, 1990, pp. 334-339.

12 V. Kek, "Bénard Konvektion in flüssigen Natriumschichten," Dr. thesis, University Karlsruhe, KfK 4611, (1989).

13 V. Kek, L. Krebs, U. Müller, "Bénard convection in liquid sodium layers," Heat Transfer 1990, Vol. 2, pp. 235-239.

14 R.M. Clever, F.H. Busse, "Low Prandtl number convection in a layer heated from below," JFM 102, 1981, pp. 61-74.

15 A. Chiffaudel, S. Fauve, B. Perrin, "Viscous and inertial convection at low Prandtl number: Experimental study," Europhysics Letters 4, 1987, pp. 555-560.

16 G. Grötzbach, "Direct numerical and large eddy simulation of turbulent channel flows," Encyclopaedia of Fluid Mechanics, Gulf Publ. Houston, Vol. 6, (1987), pp. 1337-1391.

17 M. Wörner, G. Grötzbach, "Analysis of semi-implicit time integration schemes for direct numerical simulation of turbulent convection in liquid metals," Notes on Numerical Fluid Mechanics, Ed. J.B. Vos, A. Rizzi, I.L. Ryhming, Vol. 35, pp. 542-551, Verlag Vieweg, Braunschweig, 1992.

18 C.-H. Moeng, R. Rotuno, "Vertical-velocity skewness in the buoyancy-driven boundary layer," J. Atmos. Sc. 47, 1990, pp. 1149-1162.

19 G. Grötzbach, "Simulation of turbulent flow and heat transfer for selected problems of nuclear thermal-hydraulics," Proc. Conf. on Supercomputing in Nuclear Applications, Mito, Japan, 1990, pp. 29-35.

20 Z. Kawara, I. Kishiguchi, I. Michiyoshi, "Characteristics of plumes in turbulent thermal convection in a horizontal fluid layer," Heat Transfer 1990, Vol. 2, pp. 537-542.

21 J.W. Deardorff, G.E. Willis, "Investigation of turbulent thermal convection between horizontal planes," J. Fluid Mech., Vol. 28, (1967), pp. 576-704.

Tab. 1: Case specifications and computational effort.
$N_i$ = node numbers horizontally, $N_3$ = node number vertically,
$N_t$ = number of time steps on this finest grid, CPU-time on VP 400, number of data stored permanently

| Pr | Ra | Gr | $N_i$ | $N_3$ | $N_t$ | CPU [h] | data stored [GB] |
|---|---|---|---|---|---|---|---|
| 0.006 | $3 \cdot 10^3$ | $5 \cdot 10^5$ | 128 | 31 | 17,000 | 32 | 0.15 |
| 0.006 | $6 \cdot 10^3$ | $1 \cdot 10^6$ | 200 | 31 | 16,000 | 12 | 0.45 |
| 0.006 | $12 \cdot 10^3$ | $2 \cdot 10^6$ | 250 | 39 | 40,000 | 60 | 5.1 |
| 0.006 | $24 \cdot 10^3$ | $4 \cdot 10^6$ | 250 | 39 | 23,000 | 34 | 1.2 |
| 0.71 | $630 \cdot 10^3$ | $8.9 \cdot 10^5$ | 200 | 39 | 16,000 | 18 | 2.6 |

Tab. 2: Nusselt numbers from experiments[12,13,21] and simulation results for Nu, for the maximum of the variance of the temperature fluctuations and their flatness at midplane, and estimates of the macroscopic wavelengths of the velocity field.

| Pr | Ra | $Nu_{Exp}$ | Nu | $\sqrt{\overline{T'^2}}/\Delta T_w$ | $\overline{T'^4}/(\overline{T'^2})^2$ | $\lambda$ |
|---|---|---|---|---|---|---|
| 0.006 | $3 \cdot 10^3$ | 1.05 | 1.012 | 3.6 | 1.51 | 2.5 |
| 0.006 | $6 \cdot 10^3$ | 1.10 | 1.04 | 6.3 | 1.78 | 2.6 |
| 0.006 | $12 \cdot 10^3$ | 1.19 | 1.15 | 11.8 | 1.68 | 2.6 |
| 0.006 | $24 \cdot 10^3$ | 1.49 | 1.36 | 17.0 | 1.58 | 2.7 |
| 0.71 | $381 \cdot 10^3$ | | 6.2 | 15.3 | 3.42 | 3.5 |
| 0.71 | $630 \cdot 10^3$ | 4.5-7.3 | 7.2 | 14.7 | 3.37 | 3.6 |

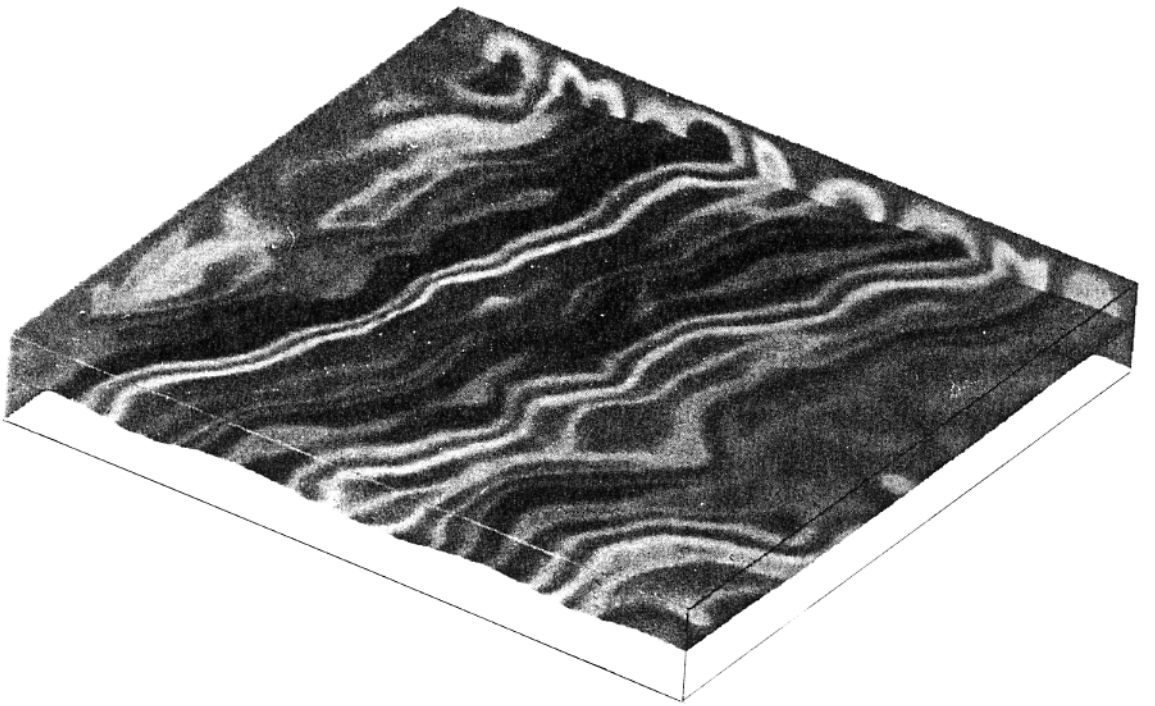

Fig. 1: Isosurface for temperature T = 0.5, colour code for vertical velocity, Ra = 3,000, Pr = 0.006.

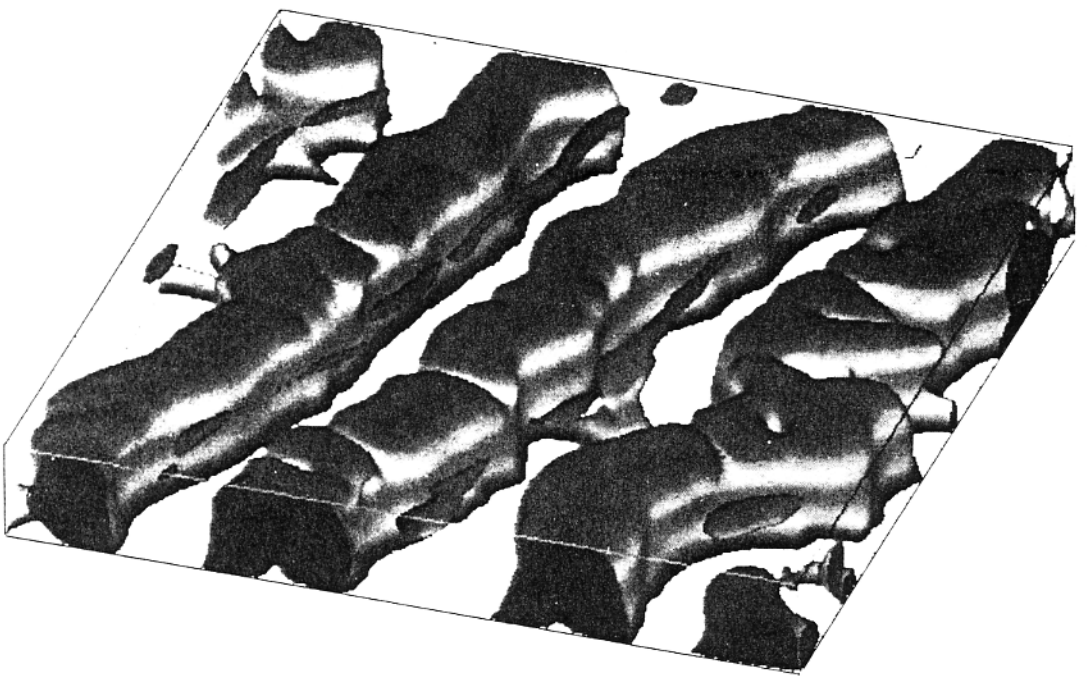

Fig. 2: Isosurface for vertical velocity $u_3 = 0.001$, colour code for temperature, Ra = 3,000, Pr = 0.006.

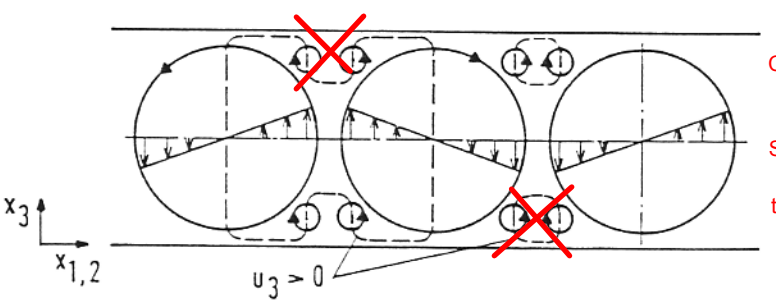


Comment after the meeting, not contained in Proc.:

Secondary vortices exist only in the wall detaching area, not in the impingment area, see PhD. thesis by M. Wörner 1994

Fig. 3: Sketch of fly-wheel vortex system with secondary vortex rolls. The dashed line denotes the position of an isosurface for $u_3 > 0$.

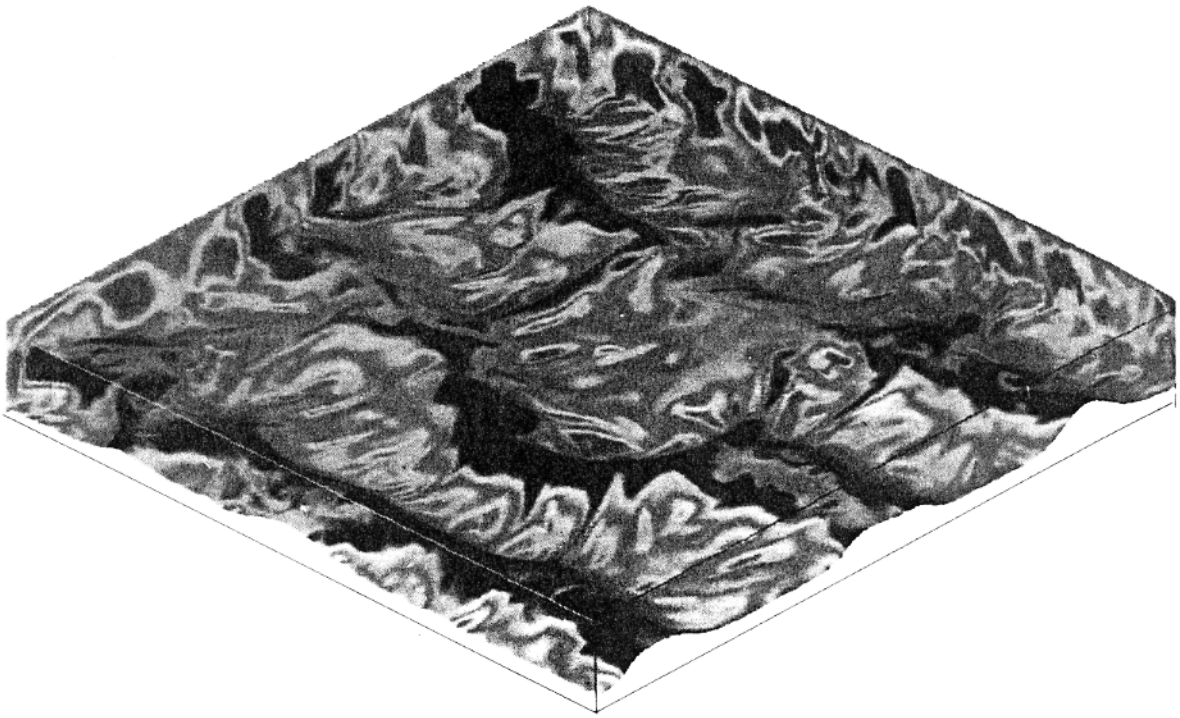

Fig. 4: Isosurface for temperature T = 0.5, colour code for vertical velocity, Ra = 12,000, Pr = 0.006.

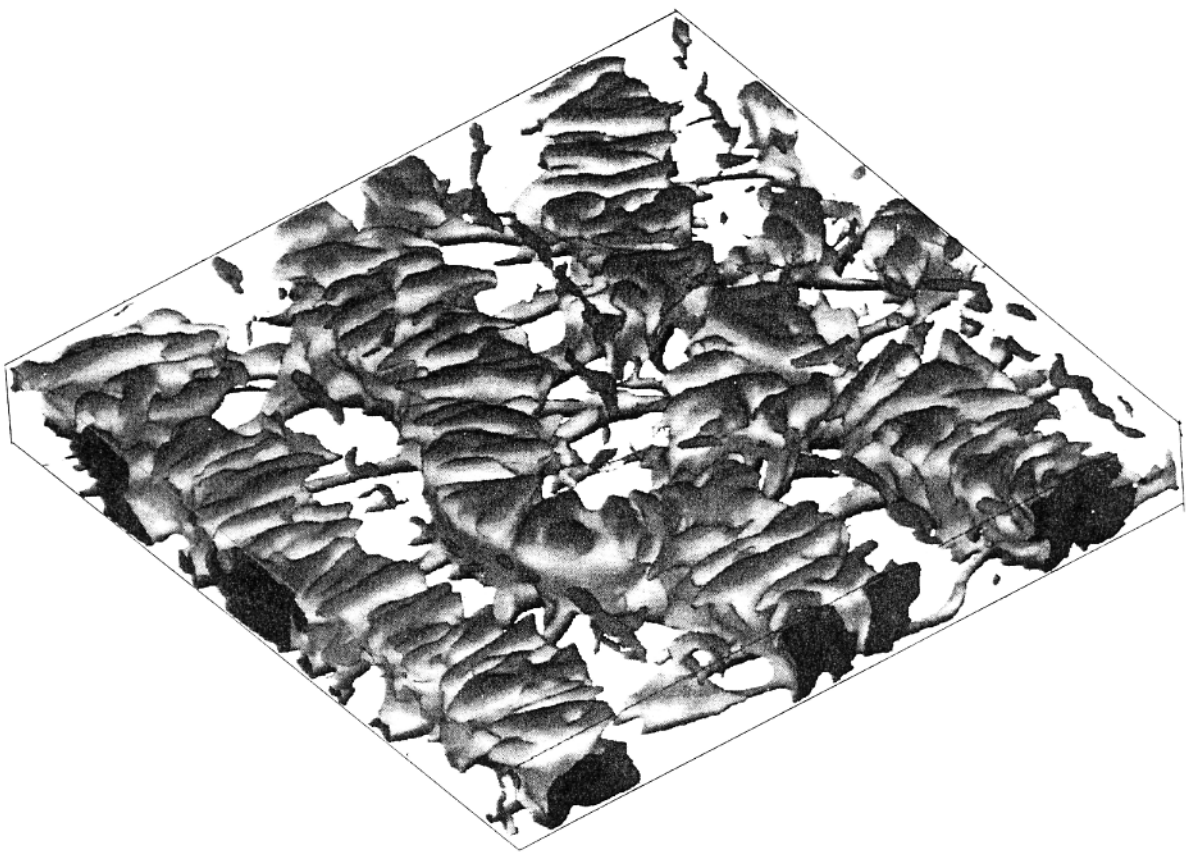

Fig. 5: Isosurface for vertical velocity $u_3 = 0.05$, colour code for temperature, Ra = 12,000, Pr = 0.006.

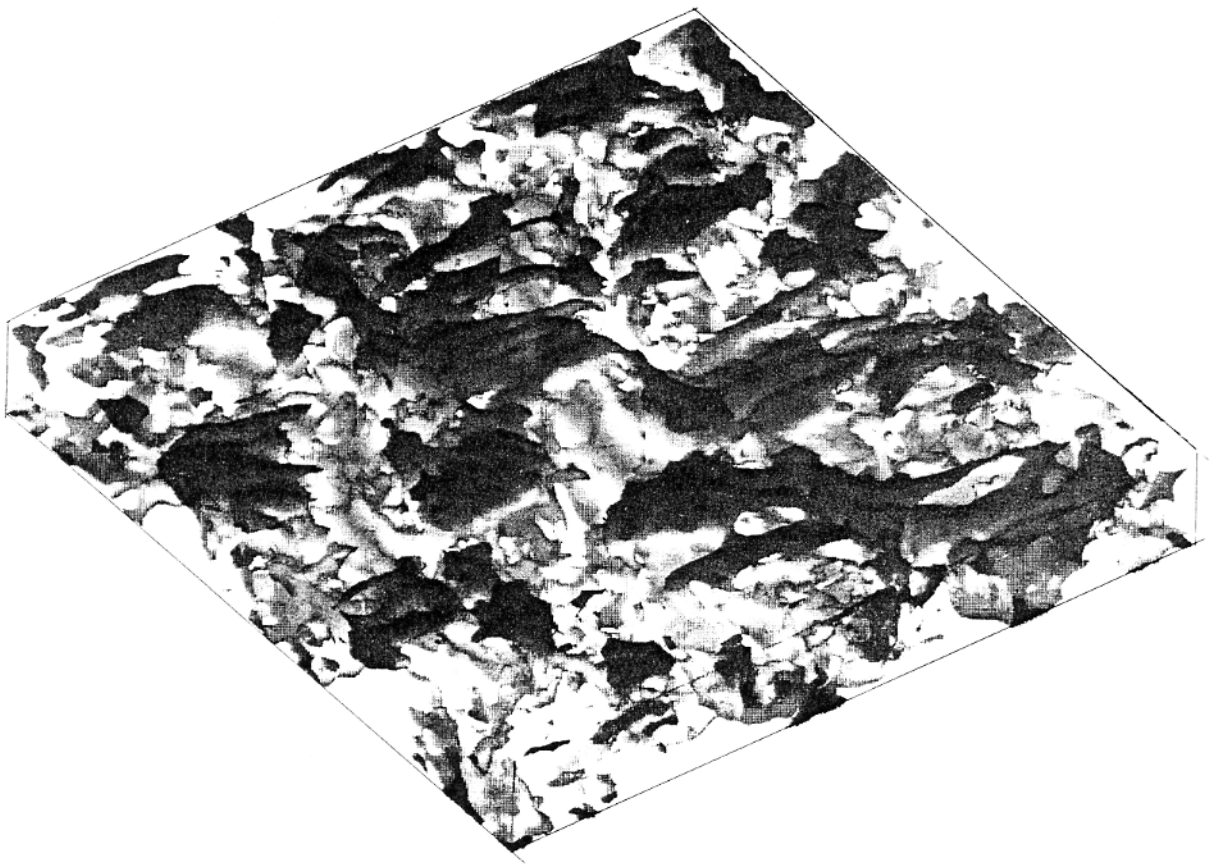

Fig. 6: Isosurface for vertical velocity $u_3 = 0.1$, colour code for temperature, Ra = 24,000, Pr = 0.006. For plotting only each second mesh cell was used.

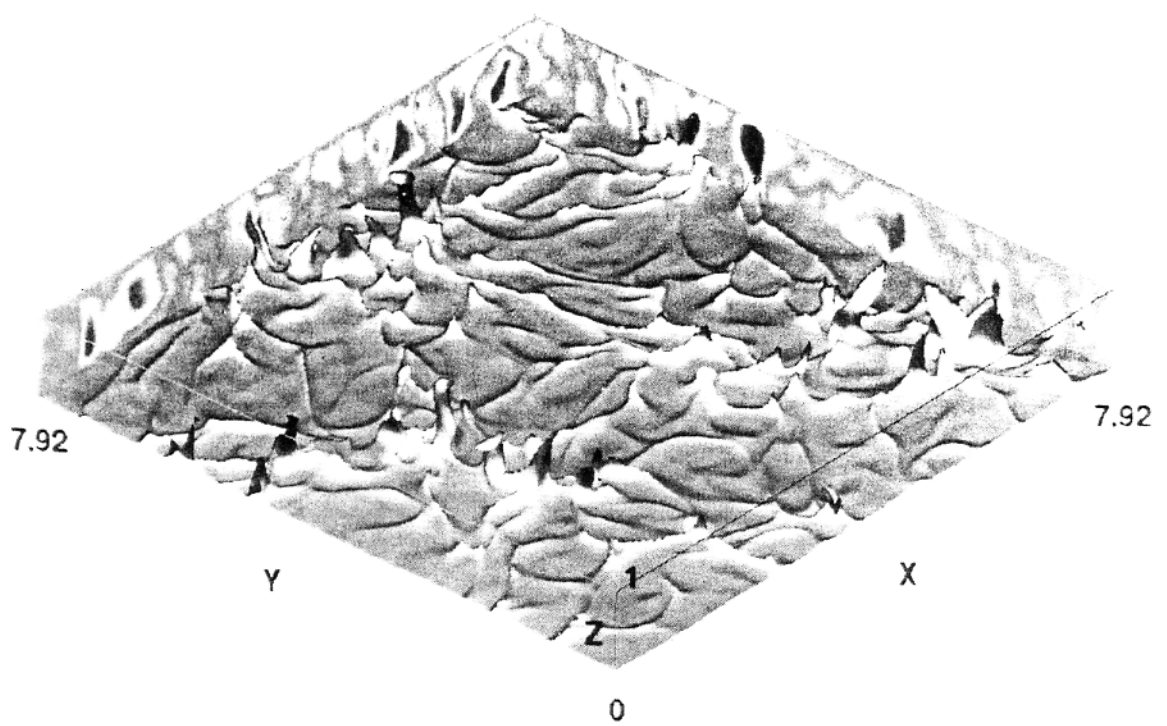


Fig. 7: Isosurface for temperature T = 0.7, colour code for vertical velocity, Ra = 630,000, Pr = 0.71.

Proceedings of the Joint International Conference on

# MATHEMATICAL METHODS AND SUPERCOMPUTING IN NUCLEAR APPLICATIONS

## M&C + SNA'93

April 19-23, 1993
Congress and Exhibition Centre
Karlsruhe, Germany

## Volume 1

Editors

**H. Küsters, E. Stein, W. Werner**

Kernforschungszentrum Karlsruhe GmbH, Karlsruhe

**Impressum**

Editors:
Dr. H. Küsters, E. Stein
Kernforschungszentrum Karlsruhe GmbH
Postfach 3640
W-7500 Karlsruhe 1
FRG

Dr. W. Werner
Gesellschaft für Anlagen- und Reaktorsicherheit mbH
Forschungsgelände
W-8046 Garching
FRG



Date published: April 1993

ISBN 3-923704-11-9

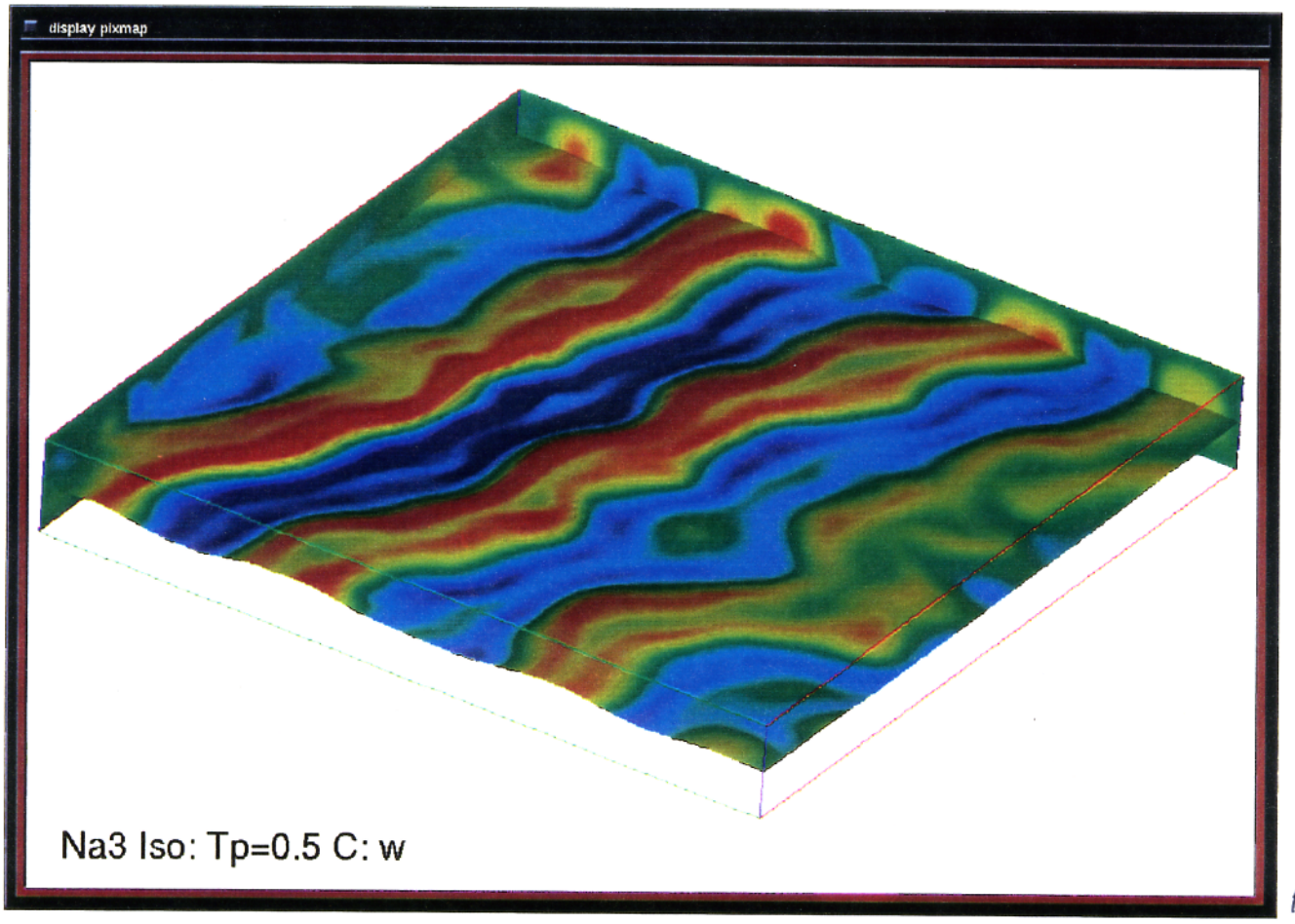


Fig. 1

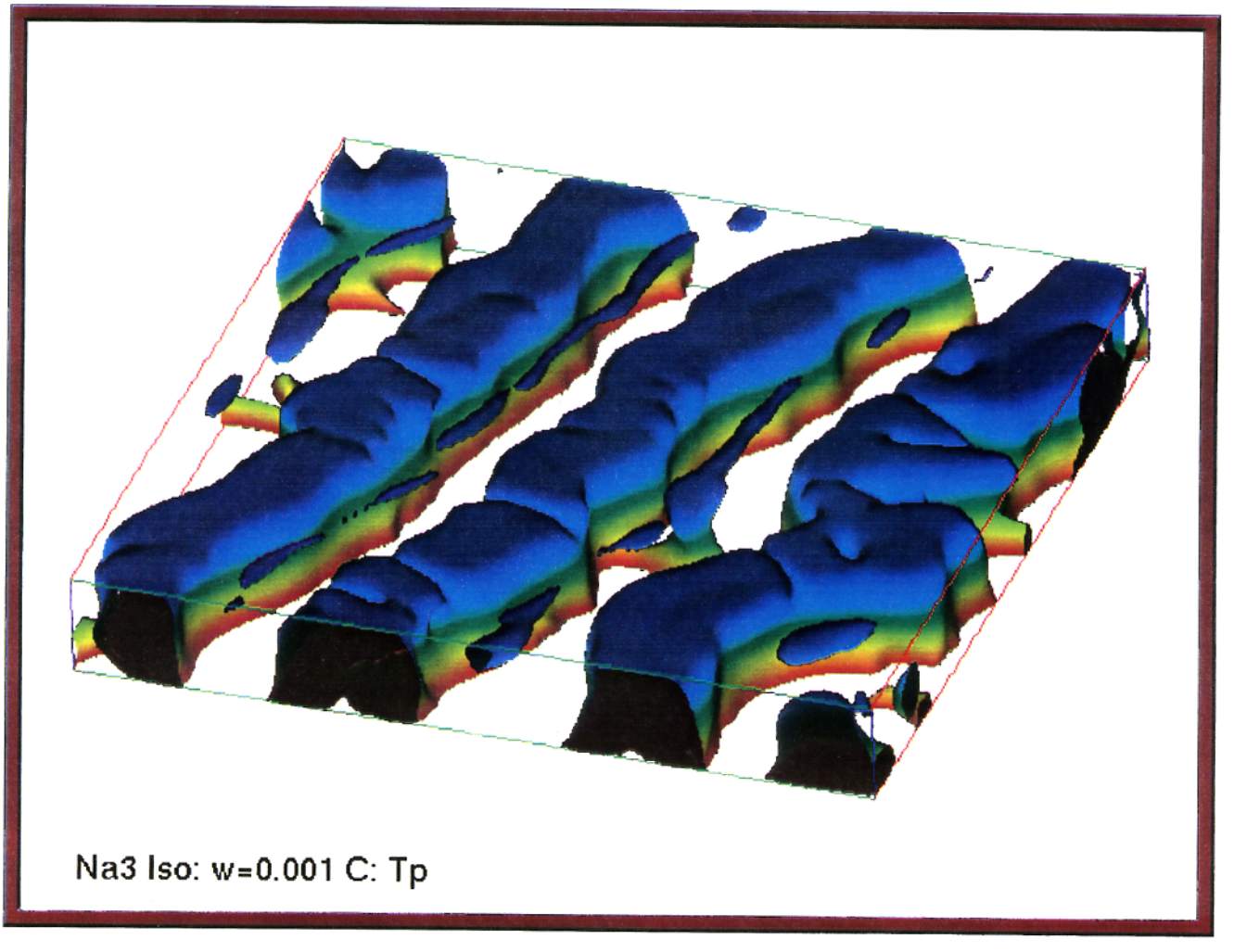


Fig. 2

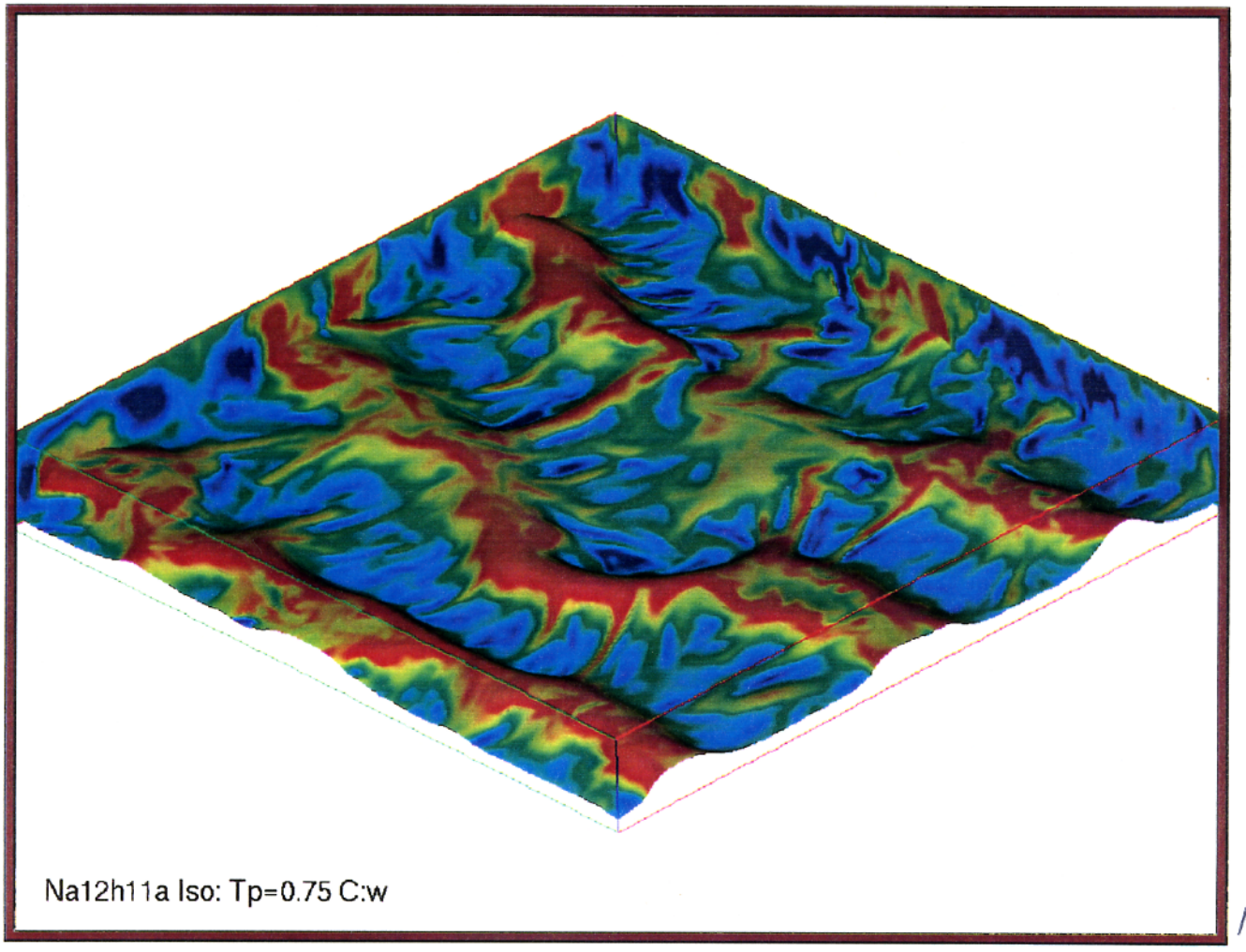


Fig. 4

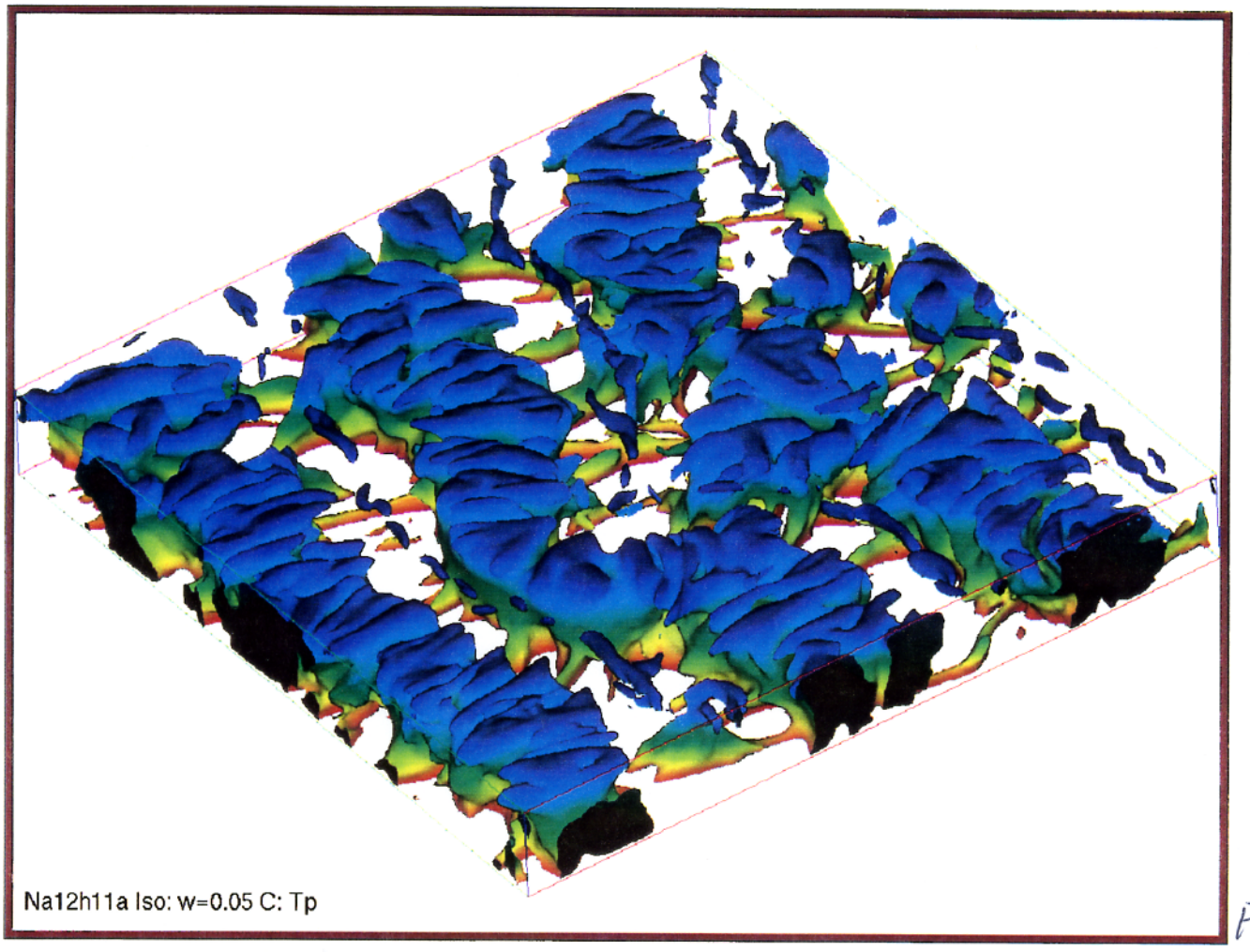


Fig. 5

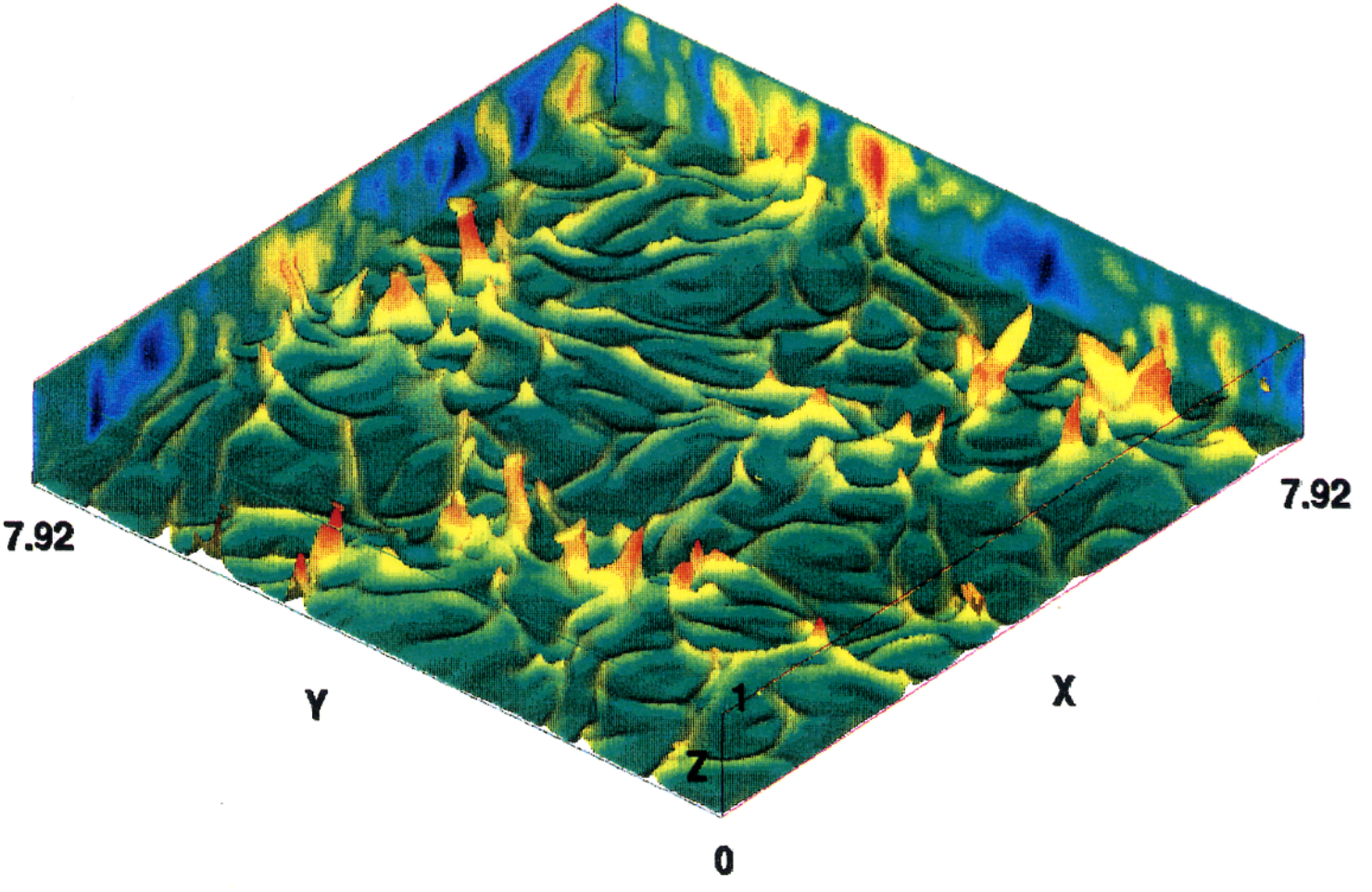


Rayleigh–Benard convection of air (BLU7) Iso: Tp=0.75 C: u3

Fig. 6